

# Low-Density Polyethylene Depth Profile Analysis by Photoacoustic Spectroscopy

MARCELO GANZAROLLI DE OLIVEIRA,\* OSVALDO PESSOA JR.,<sup>†</sup> HELION VARGAS,<sup>†</sup> and FERNANDO GALEMBECK,\*  
*Institutos de Química\* e de Física,<sup>†</sup> Universidade Estadual de  
Campinas, CP 6154 13083 Campinas SP, Brasil*

## Synopsis

Near-infrared photoacoustic spectra of polyethylene (1 mm slab) were taken in the modulation range 10–240 Hz, which corresponds to thermal diffusion layers in the 56–11  $\mu\text{m}$  range. Thick-layer spectra are very similar to polyethylene film transmission spectra, but large differences are observed between the spectra taken at various modulation frequencies. From 10 to 80 Hz, all the spectral band intensities decrease linearly with  $\omega^{-\alpha}$  where  $\omega$  is the light modulation frequency and  $\alpha$  varies from 0.48 to 1.00 for different constituent groups. The analysis of spectral intensity as a function of modulation frequency shows that peak intensity ratios of  $-\text{CH}_3$ ,  $=\text{CH}_2$ , and  $-\text{OH}$  groups, relative to that of methylene groups, increase as thinner, closer-to-surface polymer layers are sampled. From this we conclude that near-to-surface layers of solid polyethylene are richer in  $-\text{CH}_3$ ,  $=\text{CH}_2$  and  $-\text{OH}$  groups than the polymer bulk.

## INTRODUCTION

Spectroscopic methods have had a major role in the study of the composition and structure of the surface layers of solid polymers. Surface-specific methods are useful in structural studies related to adhesion, corrosion, lubrication, adsorption, and biocompatibility of polymers.<sup>1–5</sup>

Photoacoustic spectroscopy (PAS) is a technique for the detection of light absorption which samples just the surface layers of the solid or liquid under examination, down to some tens of microns beneath the irradiated surface.

Detailed experimental descriptions of PAS are in the literature;<sup>6–11</sup> extensive theoretical work is also available, to allow interpretation of PA spectra.<sup>6,12,13</sup>

The technique offers some advantages over infrared (IR) reflectance techniques (ATR, MIR):<sup>1,11,14,15</sup> sample preparation is minimum allowing the examination of opaque, hard, and insoluble solids without using abrasion or milling. Moreover, the thickness of the sampled layer may be changed by changing the light modulation range. PAS has, thus, the unique ability to give a depth profile of the chemical composition of a solid or liquid.<sup>1,7,15,17</sup>

This technique has been used in polymer analysis by many authors with the following objectives: determination of vinyl acetate in polyvinyl chloride/polyvinyl acetate copolymer;<sup>18</sup> quantitative examination of polyester-cotton;<sup>19</sup> monitoring of conjugation structures and carbonyl group formation during photo- and thermal degradation of poly(vinyl chloride);<sup>20</sup> study of natural weathering of polyethylene and of the polymer degradation mechanism;<sup>21</sup> evaluation of maximum analytical depths for PAS and ATR techniques in

thin films of polystyrene on poly(methylmethacrylate).<sup>7</sup> Gardella et al.<sup>1</sup> have compared ATR and PAS methods for improvement of the surface sensitivity in Fourier transform IR (FT-IR) analysis of polymer surfaces on commercially available biocompatible polymer mixtures and showed that both methods allow the detection of surface impurities and segregation of specific polymer components in a near-to-surface region; the degree of surface segregation was estimated by varying the sampling depth. Schneider et al.<sup>10</sup> studied the interference effects in PA spectra of polymer samples with a layered optical structure, showing that strongly absorbing layers imbedded in a polymer sample can produce a PA response via a thermoelastic effect. Other applications to polymer materials are found in Refs. 22–25.

We have examined PA spectra of low-density polyethylene at various modulation frequencies; as we found strong differences in the spectra taken at high and low frequencies, we have done a detailed examination of these, which is reported in this work.

## EXPERIMENTAL

PA spectra were obtained with a commercial spectrometer EDT model OAS 400 fitted with a 300 W, high-pressure, short-arc xenon continuum source. This radiation source is focused onto the plane of rotation of a variable-speed rotating sector which allows source modulation at preset frequencies of 10, 20, 40, 80, 160, and 240 Hz. Spectra were recorded at these frequencies, in the near IR (N/R) range 1.2–2.8  $\mu\text{m}$ . Monocromator scan rate was 0.2  $\mu\text{m}$  min, time constant was selected for 1 s, and band pass was 0.032  $\mu\text{m}$ . In the instrument used PA spectra are corrected by using a split beam and a pyroelectric detector, which signal is fed to a ratiometer together with the microphone signal. The system employs an aluminium nonresonant sample cell assembly with a transparent fused silica window. The sensitivity of PA signal channel was selected for 1 mV and 300  $\mu\text{V}$  full-scale deflection for the first three and last three chopping frequencies, respectively.

Low-density polyethylene (LDPE) film, 1.0 mm slab was obtained from Poliolefinas (São Paulo). The identity of the polymer sample was verified by IR spectroscopy.

## RESULTS AND DISCUSSION

### Peak Assignments

The NIR-PA spectra of polyethylene are shown in Figure 1. The assignment of the spectral peaks was made using standard information from the literature; the basis for the assignment is in Table I.

**C-H absorption wavelengths.** Assignments for the various overtones and combinations for the fundamental C-H stretching modes are given in Table I. Following previous work in the literature, it is possible to distinguish between methyl and methylene groups by using the absorption at ca. 2.24<sup>26,28</sup> and 2.30–2.50  $\mu\text{m}$ .<sup>24,29,30</sup> Other methyl groups' absorptions are superimposed to methylene absorptions (1.19, 1.69, 1.73  $\mu\text{m}$ )<sup>26,27,31–33</sup> or to OH absorption (1.44  $\mu\text{m}$ )<sup>16,33</sup> and cannot be used to monitor methyl groups.

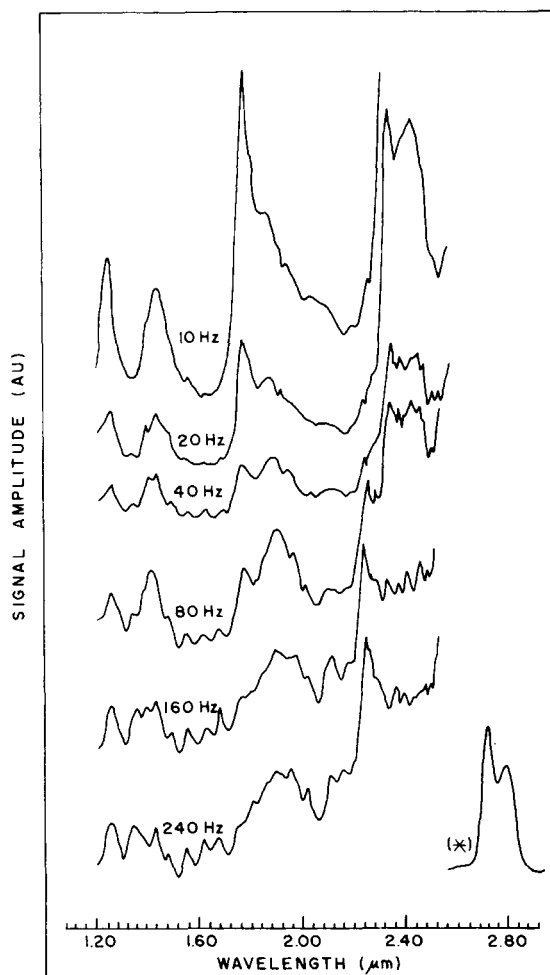


Fig. 1. NIR-PA spectra of polyethylene at six chopping frequencies. For conditions see text. \* OH absorption band of water vapor: this band has the same intensity for all chopping frequencies and was recorded at 100 mV full-scale deflection.

**Unsaturation.** Vinyl and vinylidene groups absorb in the same wavelength regions, with comparable intensities. The most useful absorptions are these at 2.1  $\mu\text{m}$  (combination) and 1.6  $\mu\text{m}$  (1st overtone of C-H stretching).<sup>28, 31, 32, 34, 35</sup> NIR-PA spectra of polyethylene presents bands at 1.62, 1.67, 2.02, and 2.08–2.16  $\mu\text{m}$ . The absorptions at higher wavelengths are characteristic of terminal vinyl groups,<sup>34</sup> but they are probably superimposed to absorption by OH groups (from —OOH and —COH);<sup>26</sup> independent contributions from hydroxo and vinyl groups cannot thus be assessed.

Bands associated with internal, *cis* unsaturations are obscured by intense C—H combination bands at 2.22–2.50  $\mu\text{m}$ , although two bands at 2.15–2.20  $\mu\text{m}$ , can be discernible in our spectra.

For these reasons, we have used absorptions at 1.62, and 1.67  $\mu\text{m}$  together with the characteristic absorptions at 1.34  $\mu\text{m}$ <sup>26, 34</sup> to monitor vinyl and vinylidene groups.

TABLE I  
 NIR-PA Absorption Band Wavelengths

	Wavelength ( $\mu\text{m}$ )	Assignment	Observation
(1)	1.25	2nd overtone	Characteristic of $-\text{CH}_2-$ and $-\text{CH}_3-$ groups
	1.42	Combination: $\nu_{\text{CH}}$ + others	" " " " " "
	1.76	1st overtone	Characteristic of $-\text{CH}_2-$ groups
	2.24	Combination: $\nu_{\text{CH}}$ + others	Characteristic of $-\text{CH}_3-$ groups
	2.30-2.48		Characteristic of $-\text{CH}_2-$ groups
(2)	1.34	Probably a combination	Characteristic of terminal olefinic methylene group
	2.02	" " "	" " " " " "
	2.08-2.14	Combination: $\nu_{\text{CH}}$ + others	" " " " " "
			Region of $\nu_{\text{OH}}$ combination band of alcohols
	2.15-2.20	" " "	Characteristic of (cis) internal unsaturation
	1.62	1st overtone	Characteristic of terminal olefinic methylene group
	1.67	" "	" "
(3)	1.36-1.40	Free OH, 1st overtone	
	1.80-1.92	Free OH, combination	
	2.71 and 2.78	Free OH, fundamental	
	1.45-1.49	Bound OH, 1st overtone	Superimposed to $\nu_{\text{CO}}$ , 3rd overtone
	1.93-2.00	Bound OH, combination	Superimposed to $\nu_{\text{CO}}$ , 2nd overtone
	2.98-3.10	Bound OH, fundamental	Superimposed to $\nu_{\text{CO}}$ , 1st overtone

(1) CH stretching modes, overtones and combinations, saturated carbon.

(2) CH stretching modes, overtone and combinations, unsaturated carbon.

(3) OH stretching modes.

Sources: Refs. 16, 24, 26-35.

**OH groups.** NIR observation of OH groups is usually made using the 1.9  $\mu\text{m}$  combination or the 1.4  $\mu\text{m}$  first overtone.<sup>30</sup> The fundamental band  $\sim 2.8$   $\mu\text{m}$  is often too intense to be conveniently used.

The spectra in Figure 1 display many bands which can be assigned to the presence of free and associated OH groups.<sup>32,33</sup> These bands may originate from OH groups bound to the polymer chain, to contaminants, to water sorbed in LDPE, and to atmospheric water vapor. Both bound (2.98-3.10, 1.93-2.00, 1.47  $\mu\text{m}$ ) and unbound (2.71, 2.78, 1.80-1.92, 1.39  $\mu\text{m}$ ) OH groups were detected. (However, note that bound  $-\text{OH}$  absorption bands are probably superimposed to other bands, assigned to CO groups, as discussed below.)

Absorption bands assigned to the 1.9  $\mu\text{m}$  combination and 1.4  $\mu\text{m}$  overtone may be compared to their neighbors, which shows a definite trend: the associated OH bands are more conspicuous as we move from low to high modulation frequencies. The opposite happens with the unbound OH bands.

Data from the literature<sup>32</sup> indicate that alcoholic OH groups may be detected in NIR by using a peak at ca. 1.55  $\mu\text{m}$ , which was also found in our spectra.

**CO groups.** The three first overtones of CO  $\nu_s$  mode may be detected in NIR spectra. However, they all superimpose to bound OH band and are thus difficult to detect, separately.<sup>17,28,31-33</sup>

### Sampling Depths

In the photoacoustic technique, the thickness of the surface layer which is under examination depends on (i) the sample thermal conductivity and (ii) the

TABLE II  
Thermal Diffusion Length ( $\mu$ ) of PE for the Light Chopping  
Frequencies Employed

$\omega$ (Hz)	$\mu$ ( $\mu\text{m}$ ) <sup>a</sup>
10	56
20	40
40	28
80	20
160	14
240	11

<sup>a</sup> Calculated using  $\alpha = 0.001 \text{ cm}^2 \text{ s}^{-1}$ .

modulation frequency of the light used. According to Rosencwaig and Gersho<sup>12</sup> the sampling depth is given by the thermal diffusion length  $\mu$ , which is the depth beneath the sample surface from which a thermal wave can propagate to the surface without being strongly attenuated:

$$\mu = \left| \frac{\alpha}{\pi \cdot \omega} \right|^{1/2}$$

where  $\alpha = K/\rho \cdot c$  is the thermal diffusivity;  $\rho$  is the density,  $c$  is the specific heat, and  $K$  is the thermal conductivity of the solid;  $\omega$  is the light modulation frequency.

Table II gives sampling depths in LDPE, as a function of  $\omega \cdot \alpha$  was taken as  $0.001 \text{ cm}^2 \text{ s}^{-1}$ . It should be kept in mind that  $\mu$  is not the maximum sampling depth: recent work by Saucy et al.<sup>15</sup> showed that PA signal in polystyrene receives some contributions from layers 2–3 times deeper than the thermal diffusion length.

Another sample characteristic which affects its signal intensity is  $l_\beta = 1/\beta$  where  $\beta$  is the absorption coefficient. For a given set of values for  $\mu$ ,  $l_\beta$  and  $l$  (sample thickness) it is possible, according to Rosencwaig and Gersho, to classify solids within six different categories:

- 1a  $l_\beta < \mu < l$ : optically transparent, thermally thin sample;
- 1b  $l_\beta > \mu > l$ : optically transparent, thermally thin sample;
- 1c  $l_\beta \gg \mu < l$ : optically transparent, thermally thick sample;
- 2a  $l_\beta < \mu > l$ : optically opaque, thermally thin sample;
- 2b  $l_\beta < \mu < l$ : optically opaque, thermally thick sample;
- 2c  $l_\beta > \mu \ll l$ : optically opaque, thermally thick sample.

PA signal intensity ( $I$ ) varies with light modulation frequency, as follows:  $I \propto \omega^{-1}$  in cases 1a, 1b, 2a, 2b;  $I \propto \omega^{-3/2}$  in cases 1c and 2c.  $I$  is proportional to  $\beta l$  in cases 1a and 1b, to  $\beta \mu$  in cases 1c and 2c, and is independent of  $\beta$  in cases 2a and 2b; in this last case the signal is said to be saturated; saturation is the source of spectral distortion and should be properly taken care of.<sup>36,37</sup> Neglect of this point may be a source of disagreement between PA and reflectance spectra.<sup>14,38,39</sup>

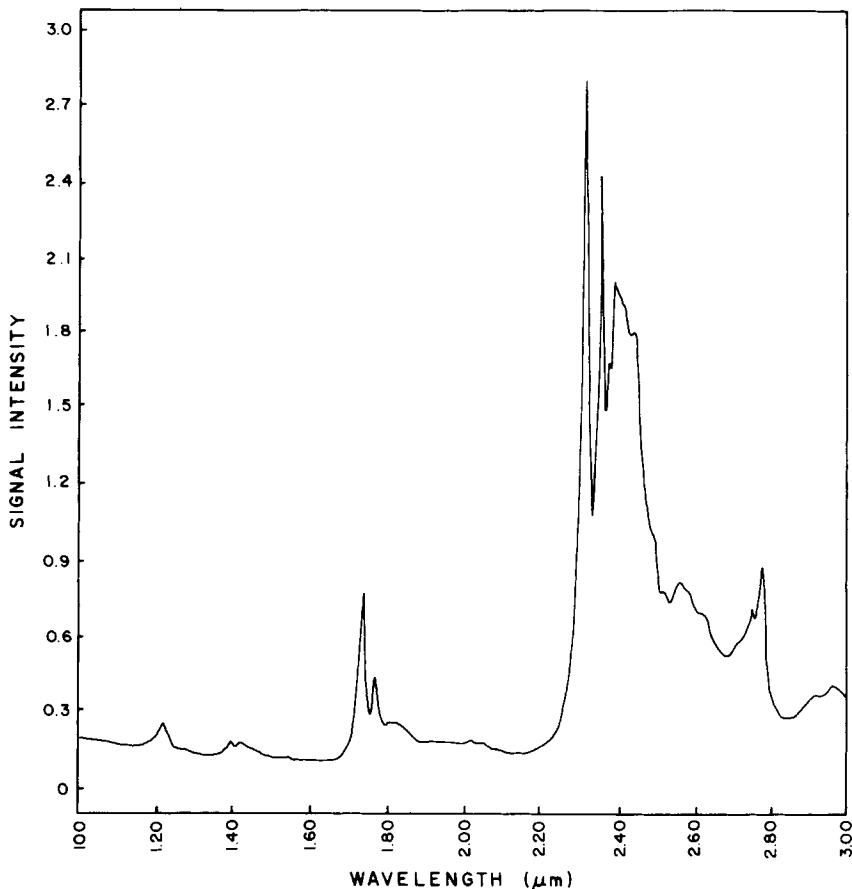


Fig. 2. NIR transmission spectrum of polyethylene (1 mm slab).

Saturation may arise when  $l_{\beta} < \mu$ . In the present case, we have evaluated  $l_{\beta}$  (as a function of  $\lambda$ ) by taking the near-infrared transmission spectrum of polyethylene (Fig. 2). The lowest  $l_{\beta}$  found was equal to  $156 \mu\text{m}$ , corresponding to the most intense ( $\lambda = 2.32 \mu\text{m}$ ) absorption peak. On the other hand, for the  $\omega$  values used in this work,  $\mu$  varies from 11 to  $56 \mu\text{m}$ , in polyethylene (Table II). Saturation is thus excluded. Other, less intense absorption peaks have  $l_{\beta}$  in the range 1–2 mm; since the sample is 1 mm thick, it is optically opaque or transparent, depending on the specific  $\lambda$  used. Moreover, since  $\mu$  is always less than  $l$ , it is thermally thick, and thus behaves as case 1c or 2c, in Rosencwaig's classification; the PA signal intensity should thus be a linear function of  $\omega^{-3/2}$  in our spectra.

In the above analysis, it has been assumed that  $\alpha$  is uniform, as we move from the polymer surface to its bulk. However, the qualitative differences observed in the spectra and published data on the crystallinity of polyethylene surfaces<sup>38-40</sup> make clear that there are differences in the physicochemical characteristics of polyethylene bulk and surface layers. One should thus be ready to accept that  $\alpha$  is a function of the polyethylene sample depth. The

expected  $\omega^{-3/2}$  dependence should not necessarily be observed in a sample of nonuniform physicochemical characteristics.

### Frequency Dependence of Band Intensities

Examination of the spectra in Figure 1 shows that different bands follow different patterns of intensity changes with frequency. Two of the most conspicuous changes are: (i) the intense band at 1.73–1.78  $\mu\text{m}$  in the low-frequency spectra appears as just a shoulder at higher frequencies; (ii) the dominating peak at higher frequencies occurs at 2.22–2.27  $\mu\text{m}$ ; it is just discernible at lower frequencies.

The 10 Hz frequency spectrum is very similar to the transmission spectrum given in Figure 2. This is to be expected, as the low-frequency spectrum

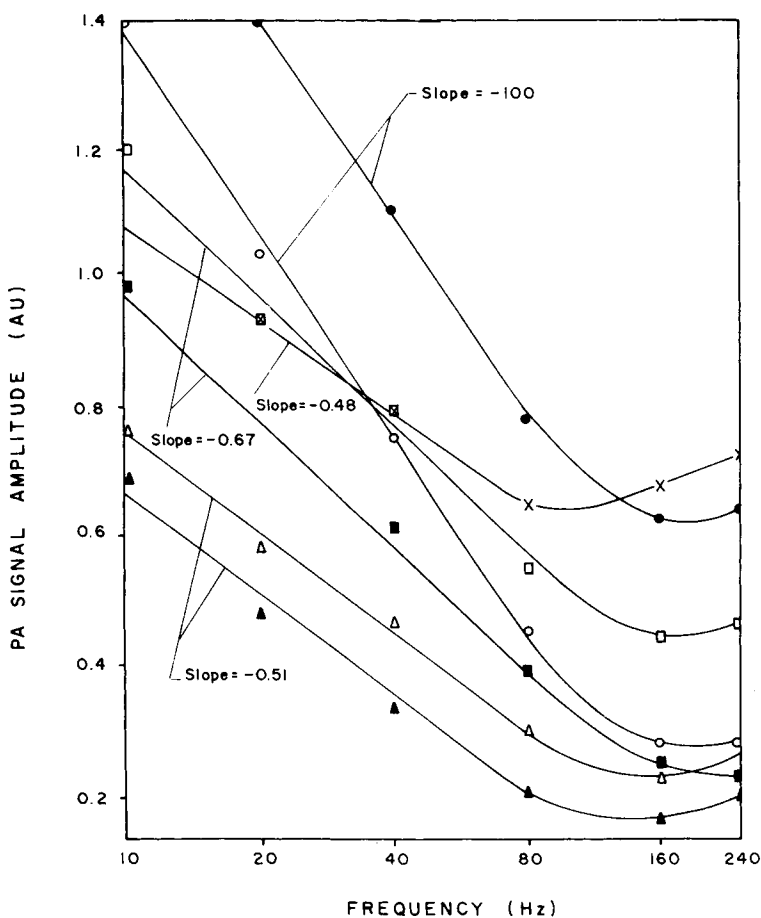


Fig. 3. Log-log plot of the PA signal for 1 mm thick PE film at various wavelengths versus chopping frequency showing different frequency dependencies for the different specific groups. (○) methylene group at 1.76  $\mu\text{m}$ ; (●) methylene group at 2.42  $\mu\text{m}$ ; (△) =CH<sub>2</sub> group at 1.34  $\mu\text{m}$ ; (▲) =CH<sub>2</sub> group at 1.62  $\mu\text{m}$ ; (□) —OH group at 1.80–1.92  $\mu\text{m}$ ; (■) —OH group at 1.39  $\mu\text{m}$ ; (×) —CH<sub>3</sub> at 2.24  $\mu\text{m}$ .

samples are deeper, having thus a greater contribution of bulk polymer than the high-frequency spectra.

Figure 3 gives plots of signal intensity as a function of modulation frequency for various absorption peaks assigned to methyl, methylene, vinyl, and hydroxyl groups. The curves have straight sections (in the 10–80 Hz range) and a concave region at higher frequencies. First, we note that in every case the slope of the curves differs for the  $-3/2$  value predicted for a sample of uniform composition by the Rosencwaig-Gersho theory. A slope less negative than  $3/2$  may be understood, assuming that the absorbing group is more concentrated at the surface than in the polymer bulk. This is likely to be correct in the case of all groups other than methylene groups, in which concentration should be rather uniform throughout the sample.

Acoustic coupling and resonance may cause slope changes and curvatures in the  $I \times \omega$  curves like those found in this work.<sup>6,13</sup> A theoretical treatment by McDonald and Wetsel<sup>13</sup> allows an evaluation of the contribution of this coupling to the PA signal. We have evaluated the contribution of this coupling (using Eq. (41) in McDonald and Wetsel's paper) to find that it is responsible for less than 1% of the measured signal, and thus irrelevant. Resonance should only occur at frequencies well above 240 Hz, the maximum used in this work.

From the fact that methylene group signal intensities decrease with a slope greater than  $-3/2$ , which is independent of the chosen wavelength, we conclude that thermal properties (i.e.,  $\alpha$ ) of the solid polymer are not uniform, as a function of the distance from the surface. We conclude also that  $-\text{OH}$ ,  $=\text{CH}_2$ , and  $-\text{CH}_3$  groups have higher concentrations at the polymer surface than at its interior. For the reasons given above, the higher the slope, the greater is the concentration gradient normal to the surface; this is thus largest for  $-\text{CH}_3$  groups and less for  $=\text{CH}_2$  and  $-\text{OH}$  groups.

### Band Intensity Ratios

To study the frequency dependence of the absorption intensities assigned to the various groups found in polyethylene, we define  $\rho(\lambda_1/\lambda_2, \omega)$ :

$$\rho(\lambda_1, \lambda_2, \omega) = \frac{\frac{\text{absorption intensity at } \lambda_1, \omega}{\text{absorption intensity at } \lambda_2, \omega}}{\frac{\text{absorption intensity at } \lambda_1, \omega = 10 \text{ Hz}}{\text{absorption intensity at } \lambda_2, \omega = 10 \text{ Hz}}} \quad (2)$$

where  $\lambda_1$  and  $\lambda_2$  are different wavelengths and  $\omega$  is the modulation frequency. Plots of  $\rho(\lambda_1, \lambda_2, \omega)$  as a function of  $\omega$  are given in Figures 4 and 5. In these curves are also indicated the respective absorbing groups.

From the curves in Figures 4 and 5, we notice that the intensity ratios for the various absorptions assigned solely to methylene groups, relative to each other, show little deviation from unity. On the other hand, absorptions of  $\text{CH}_3$  and  $\text{OH}$  groups are more intense at the higher than at the lower modulation frequencies, when compared to absorptions of methylene groups.

$\rho$  Values for two bands assigned to  $=\text{CH}_2$  groups also show little deviation from unity.  $\rho$  Values for bands assigned to associated and nonassociated



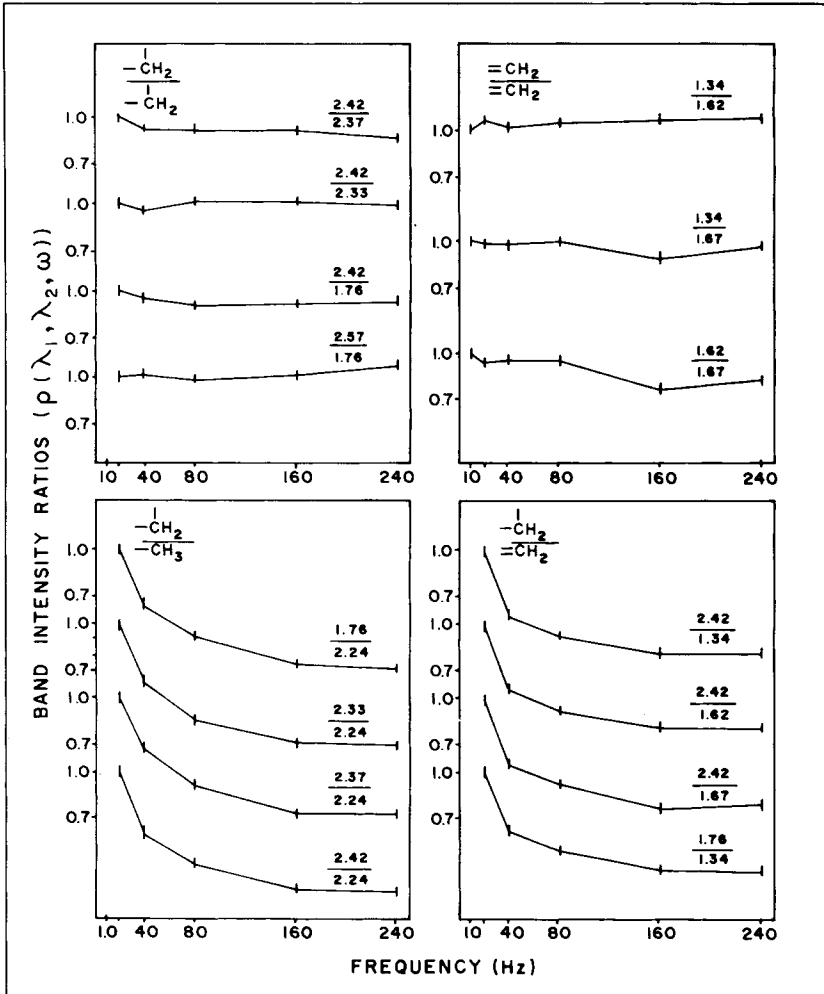


Fig. 4. Plots of band intensity ratios ( $\rho(\lambda_1, \lambda_2, \omega)$ ) versus chopping frequency. The numbers over each curve designate the wavelength ( $\mu\text{m}$ ) of the ratioed spectral bands. The Y axis has the same scale for all plots.

—OH groups show large deviations from unity, suggesting that the nature and distribution of these groups vary considerably from surface to bulk solid.

### Reasons for Polyethylene Nonuniformity

The results described in this paper lead to the following conclusions:

1. Polyethylene thermal conductivity is nonuniform, and changes as a function of depth;
2. The concentration of methyl, vinyl, and hydroxyl groups increases, as we move from the polymer bulk to the polymer surface;
3. PAS is a depth-sensitive technique. When used in polymer analysis, attention should be paid to sample characteristics which may affect surface

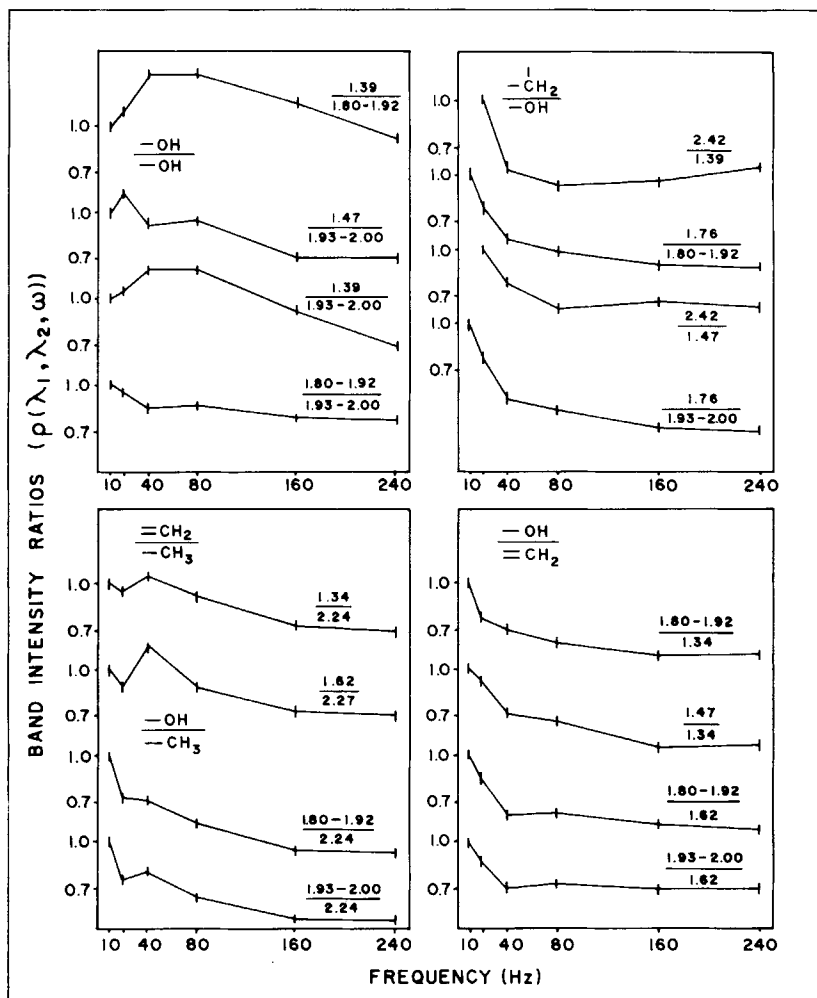


Fig. 5. Plots of band intensity ratios ( $\rho(\lambda_1, \lambda_2, \omega)$ ) versus chopping frequency. The numbers over each curve designate the wavelength ( $\mu\text{m}$ ) of the ratioed spectral bands. The Y axis has the same scale for all plots.

layers composition and thermal properties: additives, segregated low MW material, contaminants, etc.

From the measurements reported in this paper, we conclude that polyethylene surface is richer in  $\text{-CH}_3$  and  $\text{=CH}_2$  groups than is its bulk. This may be understood assuming that the surface is richer in low MW and/or highly ramified chains. This is strongly supported by data on the existence of weakly bound layers (WBL) in polyethylene from studies on polyethylene adhesion to other materials.<sup>41</sup> These WBLs are believed to be responsible for the difficulties of polyethylene adhesion, as they are peeled-off together with the adhesive or adherend applied onto polyethylene. The reason for this weakness is assumed to be the presence of low MW, waxy, noncrystalline material at the polymer surface, as indicated in the PA spectra.

Hydroxyl groups are also more highly concentrated at the surface layers than in the polymer bulk; however, their concentration gradient is less than that of the methyl groups.

This may be understood considering that: (i) —OH groups should arise from polymer oxidation, due to exposure to air, light, radiation, etc., in the slab fabrication process and storage; oxidation should thus be more intense at the surface than in the polymer bulk; (ii) —OH and any other polar groups in polyethylene in contact with air tend to move away from the polymer surface to achieve minimum surface tension; this has been well demonstrated by Baszkin et al.<sup>42</sup> Together, these two arguments lead to the conclusion that —OH group concentration should increase from polymer bulk to surface but not as fast as the concentration of groups (as —CH<sub>3</sub>) which contribute to a surface tension lowering of polyethylene.

There are some points raised in this work which should be the object of more detailed experimentation and theoretical work before they can be well understood. Some points under scrutiny at this time are: a quantitative evaluation of the thermal diffusion coefficient and concentration gradients; the bound and unbound —OH groups; the selective detection of contaminants and additives. Progress along these lines would make PAS a still more important technique for polymer study.

MGO held a FAPESP graduate fellowship. We thank Dr. Elizabeth B. Stucchi (Unesp, Araraquara) for the NIR transmission spectrum.

### References

1. J. A. Gardella, G. L. Grobe, W. L. Hopson, and E. M. Eyring, *Anal. Chem.*, **56**, 1169 (1984).
2. J. A. Gardella, J. S. Chen, J. H. Magill, and D. M. Hercules, *J. Am. Chem. Soc.*, **105**, 4536 (1983).
3. D. T. Clark, *Pure & Appl. Chem.*, **54**, 415 (1982).
4. J. C. Ericksson, C. G. Gölander, A. Baszkin, and L. ter-Minassian Saraga, *J. Colloid Interface Sci.*, **100**, 381 (1984).
5. D. Briggs, *Polymer*, **25**, 1379 (1984).
6. A. Rosencwaig, *Photoacoustics and Photoacoustics Spectroscopy*, Wiley, New York, 1980.
7. M. J. Adams, A. A. King, and J. F. Kirkbright, *Analyst*, **101**, 733 (1976).
8. A. Rosencwaig, *Anal. Chem.*, **47**, 592 (1975).
9. M. J. Adams, and G. F. Kirkbright, *Analyst*, **102**, 281 (1977).
10. S. Schneider, M. Möller, and M. Melzig, *J. Appl. Phys.*, **56**, 1492 (1984)
11. W. D. Vidrine, *Appl. Spectroscopy*, **34**, 314 (1980).
12. A. Rosencwaig and A. Gersho, *Science*, **190**, 556 (1975).
13. F. A. McDonald and G. C. Wetsel, *J. Appl. Phys.*, **49**, 2313 (1978).
14. K. Krishnan, *Appl. Spectroscopy*, **35**, 549 (1981).
15. D. A. Saucy, S. J. Simko, and R. Lenton, *Anal. Chem.*, **57**, 871 (1985).
16. U. Haas, *Can. J. Phys.*, **64**, 1063 (1986).
17. M. G. Rackley, *Chem. Phys. Lett.*, **75**, 370 (1980).
18. G. F. Kirkbright and K. R. Menon, *Anal. Chim. Acta*, **136**, 373 (1982).
19. C. M. Ashworth, G. F. Kirkbright, and E. M. Spillane, *Analyst*, **108**, 1481 (1983).
20. M. E. Abu-Zeid, E. E. Nofal, M. A. Marafe, L. A. Tahseon, F. A. Abdul-Rasoul, and A. Ledwith, *J. Appl. Polym. Sci.*, **29**, 2431 (1984).
21. A. Anani, A. Mobasher, and F. A. Rasoul, *J. Appl. Polym. Sci.*, **29**, 1491 (1984).
22. C. L. Cesar, C. A. S. Lima, N. F. Leite, H. Vargas, A. F. Rubira, and F. Galembeck, *J. Appl. Phys.*, **59**, 4431 (1985).
23. F. Galembeck, C. C. Ghizoni, C. A. Ribeiro, H. Vargas, and L. C. M. Miranda, *J. Appl. Polym. Sci.*, **25**, 1427 (1980).

24. S. M. Riseman, S. I. Yaniger, E. M. Eyring, D. Macinnes, A. G. MacDearmed, and A. J. Hieger, *Appl. Spectroscopy*, **35**, 557 (1981).
25. M. E. Abu-Zeid, E. E. Nofal, L. A. Tahseen, F. A. Abdul-Rasoul, and A. Ledwith, *J. Appl. Polym. Sci.*, **29**, 2443 (1984).
26. R. F. Goddu and D. A. Delker, *Anal. Chem.*, **32**, 140 (1960).
27. R. T. Holman and P. R. Edmonson, *Anal. Chem.*, **28**, 1533 (1956).
28. R. F. Goddu, *Ad. Anal. Chem. Instr.*, **1**, 347 (1960).
29. L. Glatt and J. W. Ellis, *J. Chem. Phys.*, **19**, (1951).
30. R. M. Bly, P. E. Keener, and B. A. Fries, *Anal. Chem.*, **38**, 219 (1966).
31. K. B. Whetsel, *Appl. Spectroscopy Rev.*, **2**, 1 (1968).
32. O. H. Wheeler, *Chem. Rev.*, **59**, 629 (1959).
33. W. J. Ellis and J. Bath, *J. Chem. Phys.*, **6**, 723 (1938).
34. R. F. Goddu, *Anal. Chem.*, **29**, 1790 (1957).
35. W. Kaye, *Spectrochim Acta*, **6**, 256 (1954).
36. J. W-P. Lin, and Dudek, L. P., *Anal. Chem.*, **51**, 1627 (1979).
37. J. F. McClelland and N. Kneseley, *Appl. Phys. Letters*, **28**, 467 (1976).
38. J. R. Rasmussen, E. R. Stedronsky, and G. M. Whitesides, *J. Am. Chem. Soc.*, **99**, 4736 (1977).
39. J. P. Luongo and H. Schonhorn, *J. Polym. Sci.*, **A-2**, 1649 (1968).
40. H. Schonhorn, in *Polymer Surfaces*, D. T. Clark and W. J. Feast, Eds., Wiley, New York, (1978).
41. H. Schonhorn and R. H. Hawn, *J. Appl. Polym. Sci.*, **11**, 1461 (1967).
42. A. Baszkin, M. Nishino, and L. ter Minassian-Saraga, *J. Colloid Interface Sci.*, **54**, 317 (1976).

Received August 18, 1986

Accepted July 30, 1987